ELSEVIER

Journal of Fluids and Structures 25 (2009) 687–696

JOURNAL OF FLUIDS AND STRUCTURES

www.elsevier.com/locate/jfs

Motion of a Möbius band in free fall

T. Leweke[a,*], M.C. Thompson[b], K. Hourigan[b,c]

[a]*Institut de Recherche sur les Phénomènes Hors Équilibre—CNRS, Aix-Marseille Université, École Centrale Marseille, 49 rue Frédéric Joliot-Curie, B.P. 146, F-13384 Marseille Cedex 13, France*

[b]*Fluids Laboratory for Aeronautical and Industrial Research, Department of Mechanical and Aerospace Engineering, Monash University, Victoria 3800, Australia*

[c]*Division of Biological Engineering, Monash University, Victoria 3800, Australia*

Received 22 June 2008; accepted 23 April 2009

Abstract

A Möbius band is a three-dimensional surface with the particular feature of having only one side and one edge. A simple geometrical model consists of a circular centreline, and surface elements which are locally tangent to this line and continuously twist around it, completing one-half turn going once around the circle. From an aerodynamic perspective, such a Möbius strip presents a profile that is locally a flat plate with an angle of attack smoothly varying between -90° and 90°, and this regardless of the orientation of the object. We here present results from an experimental study of Möbius bands in free fall, focussing on the trajectory, body motion and wake dynamics. Free-fall experiments were carried out at low Reynolds numbers in a water tank, with Möbius bands made of different plastic materials, having an aspect ratio (perimeter/width) of 14. The bands are found to rapidly adopt a bluff leading edge orientation and to follow a spiral path, with an independent frequency of pitching.

Keywords: Möbius band; Free fall; Vortex shedding; Flow-induced vibration

1. Introduction

Since the first documented observations by James Clerk Maxwell of a falling strip of paper in the mid-19th century [see, e.g., Maxwell, 1990, p. 560], the problem of aerodynamic or bluff bodies falling or rising freely in a surrounding fluid has been the object of numerous studies. Many of them have dealt with the free fall of plates or discs (Willmarth et al., 1964; Field et al., 1997; Belmonte et al., 1998; Mahadevan et al., 1999; Andersen et al., 2005; Pesavento and Wang, 2006) with special attention paid to the phenomenon of autorotation (Lugt, 1983), also referred to as tumbling, observed under certain conditions. Motivations for such studies can be found in a variety of contexts, ranging from unsteady wing aerodynamics (Dupleich, 1941; Smith, 1971), over wind turbine operation (Lugt, 1983), to tree seed dispersal (McCutchen, 1977; Augspurger, 1986). Some of the studies [see the recent review by Wang (2005)] have looked at the vorticity dynamics and fluid forces that lead to a range of observed motions, such as zigzagging, spiralling, gyrating, tumbling and fluttering. A related body of work is concerned with the free fall or rise of spheres and cylinders (Jenny et al., 2004; Fernandes et al., 2005; Horowitz and Williamson, 2006, 2008), as well as with the motion of air bubbles in a liquid (Magnaudet and Eames, 2000), where similar dynamics can be observed.

*Corresponding author. Tel.: +33 4 9613 9761; fax: +33 4 9613 9709.
E-mail address: Thomas.Leweke@irphe.univ-mrs.fr (T. Leweke).

0889-9746/$ - see front matter © 2009 Elsevier Ltd. All rights reserved.
doi:10.1016/j.jfluidstructs.2009.04.007

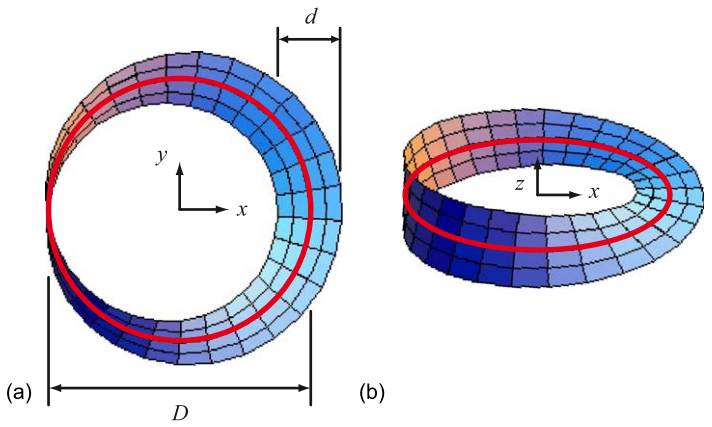

Fig. 1. Schematic of a Möbius band with a well-defined simple shape in three-dimensional space [Eq. (1)]. (a) Top view, (b) oblique view.

The present experimental study focuses on the free fall of a well-known body, the Möbius band (Fig. 1). Mathematically, this shape is famous because it has only one side and one edge. The band also possesses intriguing aerodynamic properties. When placed in a uniform flow perpendicular to the plane of the centreline, the band will locally act like a thin flat plate. Due to its particular geometry, the different elements around the band will cover all possible angles of attack, positive and negative, from perpendicular to the flow to aligned with it. One therefore encounters a range of different flow situations, from flow around streamlined bodies, over high angle of attack flows, up to bluff body wakes, all for the single object of a Möbius band. Different parts of the strip are naturally expected to experience significantly different drag forces.

If the band is not held perpendicularly to the flow, but allowed to fall freely under its own weight, it is not obvious in advance which mean orientation it will choose, since the fact that all angles of attack are present remains true, no matter from which direction the flow comes. In addition, the twisted nature of the band is likely to lead to torque forces and a resulting spinning motion, as the band moves down.

We here present a set of experimental results concerning the free fall of a Möbius band at low to moderate Reynolds numbers. The orientation, trajectory and vortex-induced oscillation of this body as it falls are described qualitatively and quantitatively, and visualisations of the vortical structures in its wake are shown. The following section gives details about the Möbius strips that were used, and the experimental set-up and techniques. The results are presented and discussed in Section 3, followed by a conclusion in Section 4.

2. Experimental details

2.1. Möbius bands

A Möbius band (or strip) is a three-dimensional surface with the particular feature of having only one side (it is non-orientable) and one edge. A simple physical model can be obtained by taking a sufficiently long rectangular strip of paper, twisting one end by 180°, and then gluing the two short ends together. This particular topological object was "invented" independently in 1858 by the German mathematicians Listing (Listing, 1861) and Möbius (Möbius, 1865). A Möbius band made from a rectangular strip will assume a complicated shape in space, depending on the aspect ratio and thickness of the initial rectangle and the elastic properties of the material (Mahadevan and Keller, 1993; Starostin and Van der Heijden, 2007). There exists, however, a simple geometrical model of a Möbius band in three-dimensional Euclidian space. It consists of a circular centreline and surface elements which are locally perpendicular to this line and continuously twist around it, completing one-half turn going once around the circle. The coordinates of points on this object are given by the following relations.

$$x(a,b)=\left(\frac{D}{2}+a\cos\frac{b}{2}\right)\cos b,\quad y(a,b)=\left(\frac{D}{2}\pm a\cos\frac{b}{2}\right)\sin b,\quad z(a,b)=a\sin\frac{b}{2}, \tag{1}$$

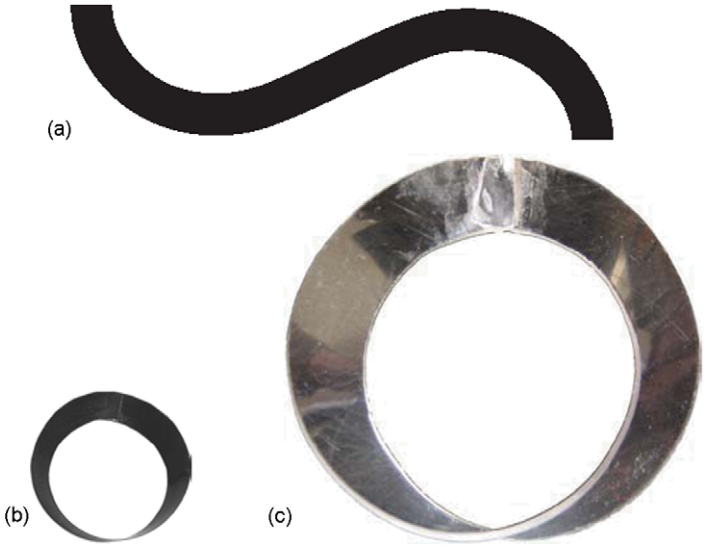

Fig. 2. (a) Shape used as an approximate development of a Möbius band of aspect ratio $A = 14$. Small (b) and large (c) bands used in this study, shown in their actual size.

Table 1
Properties of the Möbius bands.

	Möbius band 1 ("small")	Möbius band 2 ("large")
Material	Polyester	Polycarbonate
Twist direction	Negative	Positive
Thickness, h	0.12 mm	1.0 mm
Diameter, D	18 mm	45 mm
Width, d	4 mm	10 mm
Mass, m	0.0384 g	1.96 g

where the parameters a and b vary in the ranges $-d/2 \leqslant a \leqslant d/2$ and $0 \leqslant b < 2\pi$, respectively. D is the diameter of the circular centreline, and d the width of the band. The "+" or "−" sign inside the parentheses of the equation for y determines which way the surface twists as b increases. An illustration for positive twist is given in Fig. 1.

The surface defined by Eq. (1) has the disadvantage of not being developable, as shown, e.g., by Schwarz (1990). This means that, in principle, one cannot find a two-dimensional flat shape that could be twisted and glued together to give precisely this Möbius band, without stretching of the material. It was therefore decided to settle for a sufficiently close approximation of this shape, using an empirically determined developed surface. The latter was obtained with the help of a band of deformable and stretchable material (Bluetack®) which was manually shaped into a Möbius band similar to the one in Fig. 1, using a circular metal ring as a guide for the centreline. The band was then cut open and laid flat, and its shape was scanned, smoothed and symmetrised. The resulting surface [Fig. 2(a)] served as a prototype, from which the approximate developments of the bands were found by variation of the appropriate scales.

Two Möbius bands were used in the present experiments. They are shown in their actual size in Figs. 2(b) and (c), and their respective properties are listed in Table 1. The smaller one was cut out of an overhead transparency, whereas the larger one was made from a 1 mm thick transparent polycarbonate sheet.

2.2. Set-up and procedure

The free-fall experiments with the above Möbius rings were carried out in a water tank of dimensions 50 cm × 50 cm × 120 cm, with 20 mm glass walls (Fig. 3). Preliminary experiments had shown that freely falling Möbius rings of the aspect ratio used in this study would invariably orient themselves into a fairly upright position, with the blunt part facing upstream (= down), and this regardless of the orientation in which they were released. In later

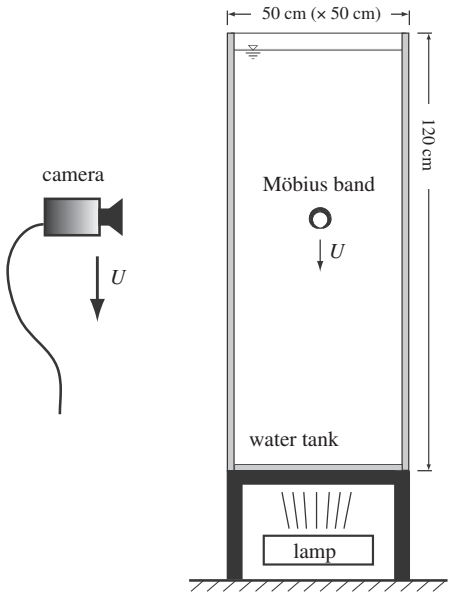

Fig. 3. Schematic of the experimental set-up.

runs, the bands were therefore released straight away in this position, just underneath the free surface near the centre of the square tank section. The interior of the tank was illuminated with either white light from a neon lamp placed underneath its glass base, for recordings of the ring dynamics and trajectories, or by the light from an argon ion laser, for visualisations using fluorescent dye painted on the bands prior to release. The motion of the falling band was recorded using a digital camera, which was either fixed or displaced vertically at about the same rate as the speed of the band. The average speed U of the strip was calculated from the time it took to fall from the free surface to the bottom of the tank 114 cm below. The frequencies characterising the time-dependent motion of the bands during their descent were obtained from analysis of the video recordings—further details are given in Section 3.

2.3. Parameters

The non-dimensional parameters governing this flow problem are:

(i) the Möbius band aspect ratio (perimeter/width), $A = \pi D/d$;
(ii) the Reynolds number, $\mathrm{Re} = Ud/\nu$, calculated with the mean sink speed U, the width d and the kinematic viscosity ν of the water ($1.054 \times 10^{-2}\,\mathrm{cm^2/s}$ at 18 °C in the present experiments);
(iii) the mass coefficient of the band, which we define here as $m' = m/(\rho D d^2)$, where ρ is the density of the water ($0.9987\,\mathrm{g/cm^3}$ at 18 °C).

The mass (inertia) of the freely falling Möbius strip is expected to have an effect on its wake-vortex-induced vibrations, similar to the case of more "standard" bodies, such as cylinders or spheres, moving through a fluid. For these configurations, the non-dimensionalisation of mass is straightforward: a mass ratio (m^*) is calculated by dividing the body mass by the mass of the displaced fluid. The same cannot be done for the Möbius strip, which is treated here as a pure surface without a volume, i.e., we assume that its thickness, and any variations of it, have a negligible effect on the flow and body motion. In order to compare the body mass to some relevant fluid mass in this situation, we choose the latter as the one contained in the simplest geometrical shape tightly surrounding the band, which is a torus of diameter D and cross section diameter d. This mass is given by $(\pi^2/4)\rho D d^2$, which we use to non-dimensionalise m. For the definition of our mass coefficient m', we drop the constant $\pi^2/4$.

The values of the three non-dimensional parameters for the two Möbius rings tested are given below at the start of Table 2.

The quantities describing the motion of the band include the mean drag coefficient, defined as $c_D = F_D/((\pi/2)\rho U^2 D d)$, where the drag force F_D is equal to the mean force pulling the band down, i.e., the difference

Table 2
Summary of measured quantities.

	Möbius band 1 ("small")	Möbius band 2 ("large")
Aspect ratio, $A = \pi D/d$	14	14
Reynolds number, $\mathrm{Re} = Ud/\nu$	130	560
Mass coefficient, $m' = m/(\rho D d^2)$	0.13	0.44
Mean drag coefficient, c_D	0.80	2.16
Spin direction	Clockwise[a]	Counter-clockwise[a]
Spin Strouhal number, St_s	0.054	0.082
Helix trajectory wavelength, D/St_s	$18.5D$	$12.2D$
Helix trajectory diameter	$1.9D$	$1.1D$
Mean angle of inclination	29°	27°
VIV Strouhal number, St_v	0.091	0.106
VIV amplitude (peak to peak)	20° (~$2d$ lateral displacement)	42° (~$4d$ lateral displacement)
Frequency ratio, f_v/f_s	7.5	5.8

[a]Looking down (upstream).

between its weight and the weight of the displaced water (buoyancy force): $F_D = (m - \rho\pi Ddh)g$ (g: acceleration of gravity). It is normalised using the dynamic pressure and the area of the strip, which we take here as πDd. The time-dependent motion can be characterised by the average frequencies of oscillations induced by vortex shedding from the blunt leading edge, and of the spinning or spiralling motion due to the torque generated by the angled lateral surfaces. These two frequencies are designated by f_v and f_s, respectively. They are non-dimensionalised to give the corresponding Strouhal numbers $\mathrm{St}_v = f_v d/U$ and $\mathrm{St}_s = f_s D/U$.

Due to the imperfections in the manufacturing of the rings and to the simple means used to analyse the flow, the errors and uncertainties in these parameters must be considered to be of the order of 3–5%.

3. Results

In this section, we present the experimental observations made for the free fall of the two Möbius bands considered in this study. Both bands have an aspect ratio $A = 14$, which is an intermediate configuration between very thin bands ($d \ll D$) and bands with a mostly blocked interior ($d > D$). The bands were made out of plastic material which is only about 20% denser than water, resulting in relatively low net body forces (weight minus buoyancy), and consequently in low falling velocities. The average descent velocities were measured as $U = 3.50$ and 5.94 cm/s, resulting in Reynolds numbers $\mathrm{Re} = 130$ and 560 for the small and large rings, respectively. The bands further differ with respect to their mass coefficient, which is almost 3.5 times higher for the larger band, due to its higher relative thickness (see Table 2). The mean drag coefficient also turns out to be quite different for the two bands. Its value is significantly higher for the large band, which is possibly linked to the higher level of vortex-induced vibrations that this body exhibits, as discussed further below.

When a Möbius band is released near the surface of the water tank, it rapidly settles into a characteristic pattern of motion. It orients itself in a way where the plane of the circular centreline is almost vertical, with the blunt edge facing down, which is close to the orientation depicted in Figs. 2(b) and (c). The trailing part of the ring just opposite is more or less aligned with the direction of motion (flow direction). The large-scale trajectory of the band is not a straight line. Instead, the body moves along an elongated helix, while at the same time spinning around a vertical axis. In addition, the band undergoes pitching oscillations in the lateral direction, perpendicular to its plane, at a significantly higher frequency than the spinning. This qualitative behaviour is the same for both Möbius bands investigated—differences were only found on a quantitative level, as shown below.

In the following, the two types of motion, as well as the resulting wake structure, are be described in more detail. All quantitative results mentioned in the text are again summarised in Table 2.

3.1. Large-scale trajectory

In Fig. 4, parts of the Möbius band trajectories are visualised by a superposition of images taken with a camera at rest. For the small strip, Fig. 4(a) clearly shows a sinusoidal lateral displacement, whereas the strip rotates at the same

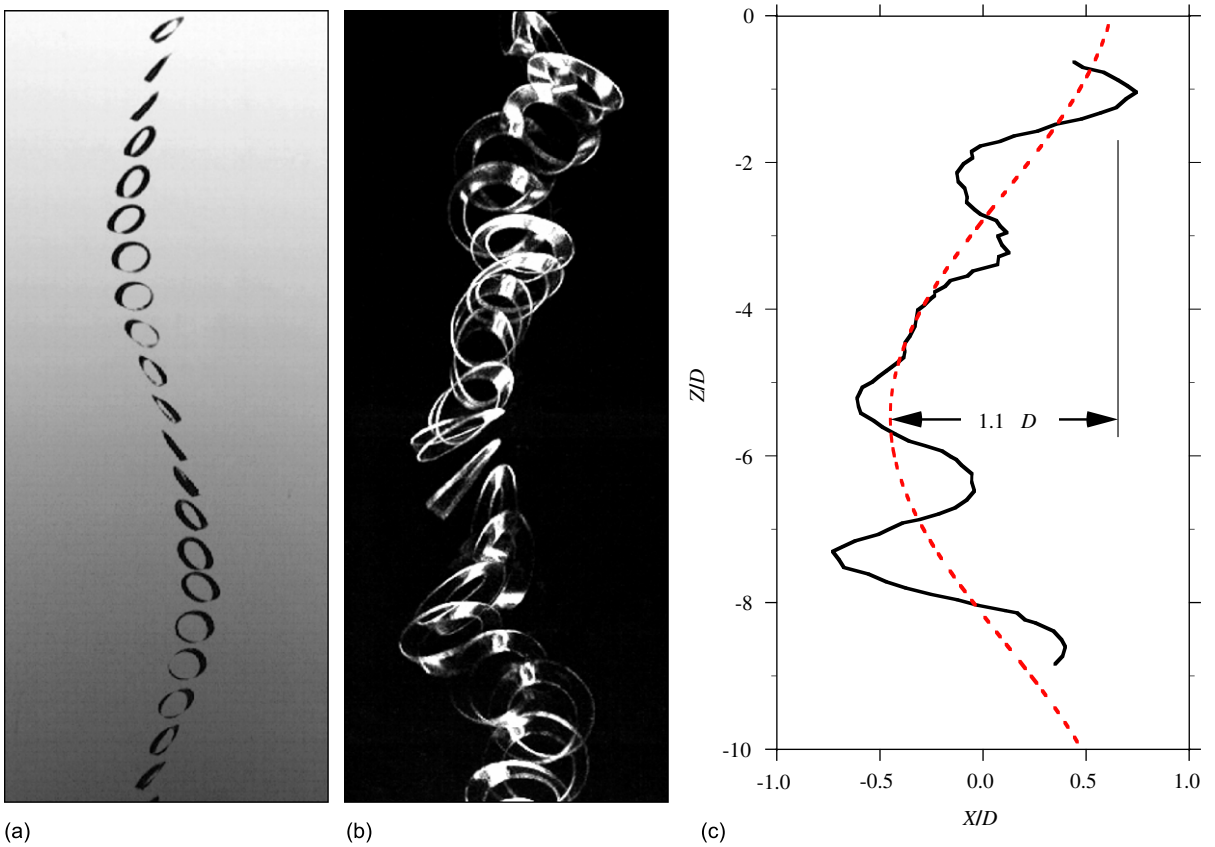

Fig. 4. Stroboscopic visualisations of trajectories of the freely falling small (a) and large (b) Möbius bands. The field of view is about $16 \times 40\,\mathrm{cm}^2$ in both cases. (c) Trajectory of the centre of the large band, for the sequence in (b). The scale in the transverse X-direction is stretched by a factor of 3 with respect to the vertical Z-direction.

time around a vertical axis. From this (and further direct observation), one can conclude that the band follows a helical path downwards. The peak-to-peak amplitude of the lateral displacement can be deduced directly from the visualisations; it amounts to $1.9D$ for the small band. The frequency f_s of spinning is found from video recordings of the body motion, by identifying the times when the band is seen under the same angle, e.g., from the side, which correspond to well-defined phases of the motion [see next section and Fig. 5(b)]. The vertical wavelength (pitch) of the helical path is given by $U/f_s = D/\mathrm{St}_s$, which for the small band is about 10 times the lateral helix diameter.

The large-scale trajectory is less visible for the large Möbius band in Fig. 4(b), since a higher frequency lateral oscillation of relatively high amplitude is superposed. From this visualisation, the precise trajectory of the band centre can be obtained; it is plotted in Fig. 4(c). Using the vertical wavelength associated with the spinning motion, determined in the same way as above, a sinusoidal mean path can be fitted to these data, shown as a dotted line. Even if only about $\frac{2}{3}$ of a cycle is captured in the field of view, one can nevertheless deduce a helix diameter of $1.1D$, which is also close to $\frac{1}{10}$ of the vertical wavelength.

The direction of the spinning motion, and the handedness (chirality) of the helical path depends on the twist direction of the Möbius band. The small band with negative twist spins clockwise, and describes a right-handed helix; the large band with positive twist does the opposite. This behaviour can be understood qualitatively from the fact that the mean position of the band is fairly vertical, with the blunt edge facing down. The surface elements on both sides induce a moment on the body, whose direction depends on the way they are angled.

3.2. Vortex-induced oscillation

Fig. 4 has already shown that, in addition to the slow spinning and large-scale spiralling trajectory, the band undergoes lateral oscillations on a smaller time scale. In Fig. 5(a), the lateral position X of the larger ring, corrected

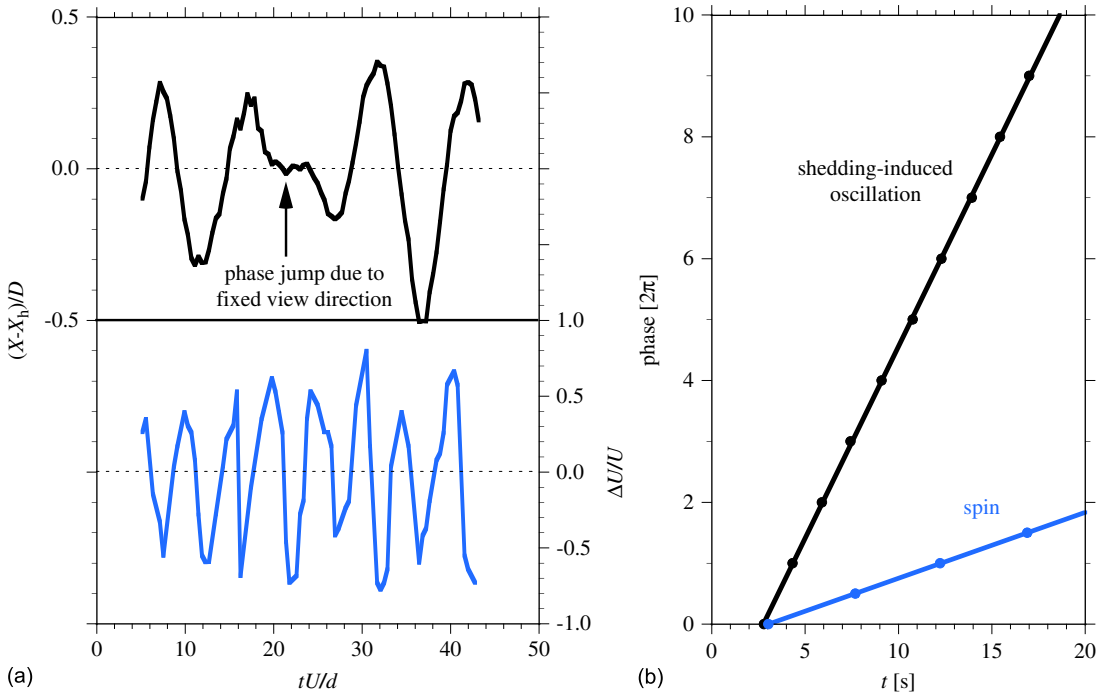

Fig. 5. (a) Top: lateral position of the centre of the large Möbius band, corrected for the average spinning motion. Bottom: difference between instantaneous and average vertical speed. (b) Phase evolution for the two types of motion observed in the free fall of the large band.

for the displacement X_h due to the large-scale helical path, is plotted as function of time, which clearly shows this oscillation. These data also reveal an apparent phase jump in this motion, which can be explained by the fact that the direction of oscillation spins with the body as it follows its spiral path, whereas the view direction remains fixed in space.

The frequency of oscillation can again be determined quite accurately from the series of times where a certain phase of this motion occurs (the maximum lateral displacement was used in this case). Fig. 5(b) shows an example of such a measurement, together with the one related to the spinning motion. The spinning and lateral oscillations are extremely regular, their frequencies are given by the slopes of the corresponding straight lines in this phase evolution plot. For both Möbius bands used here, the Strouhal number of the rapid oscillations, calculated with the width d of the bands, is close to 0.1. This is roughly in the range of values that one would expect for vortex shedding from a flat plate of width d at high angles of attack. Since the bands descend with their bluff edge facing down, it is therefore quite natural to ascribe the observed oscillations (or vibrations) to the interaction with the vortices shed from this bluff leading edge of the band. Some further evidence for this is presented in the following section.

A close-up of the actual motion performed by the Möbius bands during one cycle of oscillation is shown in Fig. 6, for the example of the large strip. The sequence starts with the band at one extreme of the lateral motion, where it is practically vertical. During the first half of the cycle (a–c), the plane of the ring tilts by an angle of about 40° until it reaches the other extreme position. During this ascending motion of the bottom edge, almost no rotation around the vertical axis takes place. This is different during the second half of the cycle (d–f), where the band, in addition to returning to its almost vertical position, rotates by about 62° around the vertical. The spinning motion is therefore found not to be constant in time, it is modulated by the vortex-induced oscillations.

The amplitude of the oscillations can be inferred from these visualisations, as seen in the superposition of images in Fig. 6(g). It is 42° from peak to peak for the large ring, and only half this value for the smaller one. This corresponds roughly to an overall lateral displacement of $4d$ and $2d$, respectively. Fig. 6(g) also shows that the mean orientation of the plane of the ring is not vertical, but inclined by slightly under 30° for both bodies. The higher relative oscillation amplitude of the larger ring is possibly the cause for its higher mean drag coefficient. During these oscillations, the ring reaches much higher inclination angles with respect to the vertical, thus exposing a higher proportion of its surface to the flow at high angles of attack (in a more vertical position, these parts are hidden behind the blunt leading edge).

During the cycle shown in Figs. 6(a)–(f), the large ring has fallen a distance of $\sim 2D$, which corresponds to about $\frac{1}{6}$ of the helix path wavelength. The ratios of spinning and oscillation frequencies were found to be of the same order for

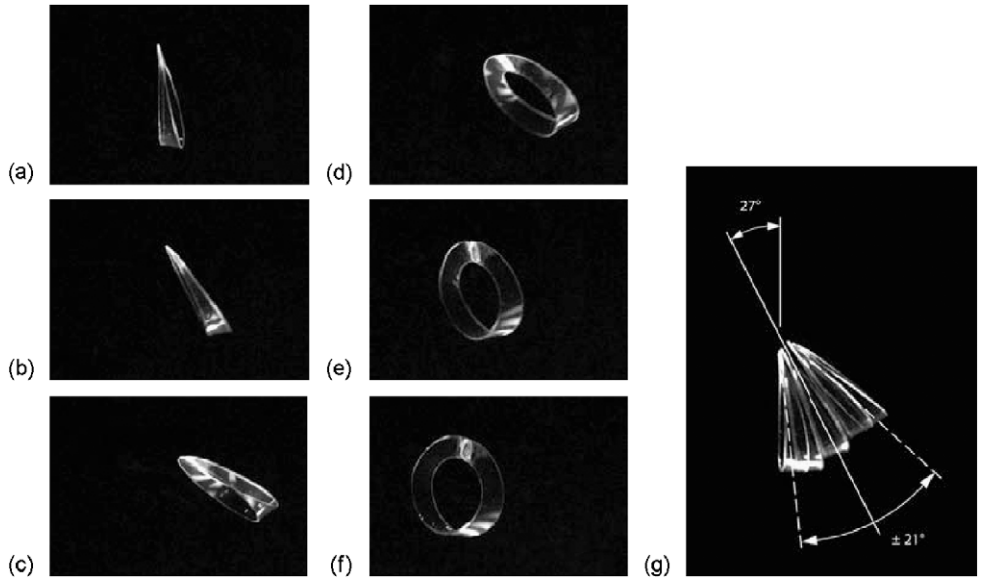

Fig. 6. (a)–(f) One cycle of vortex-induced oscillation of the large Möbius ring. Images are separated by 20% of the oscillation period. (g) Instantaneous and mean inclination of the large ring. Images from an ascending half-cycle were superposed after compensation for the vertical motion of the trailing edge.

both rings (see Table 2). Since the spinning on the helical trajectory is not actually an oscillation, but a rotation, a direct coupling between these two motions is not to be expected. There may, however, be a more subtle link. As discussed above, the spinning motion occurs mainly during the half-cycle of oscillation in which the ring returns from a very tilted position to an almost vertical one. One may conjecture that the amount of spinning is related to the amplitude of this motion, so that for higher oscillation amplitudes it takes fewer cycles to perform one spinning rotation; their number is given by the frequency ratio f_v/f_s. The present observations are consistent with this idea: the smaller ring oscillates with a lower amplitude and exhibits a slightly higher frequency ratio than the larger one.

Analysis of the ring trajectory obtained from the image sequence in Fig. 4(b) allows the determination of the instantaneous vertical velocity of the descending Möbius ring. The result is shown in Fig. 5(a): the ring speeds up and slows down by about 50% of the average descent velocity U, and this twice in every shedding cycle. Comparison with the simultaneous measurement of the lateral position reveals that the minimum descent speed occurs at the maximum lateral displacement (in either direction), whereas the highest descent speed is observed around its mean position. An observer who would follows the ring at constant speed—and who would be able to rotate around it at the spinning frequency—would therefore see the centre of the band perform a figure-of-eight trajectory, which is a well-known characteristic of vortex-induced vibrations of bluff bodies with several degrees of freedom.

3.3. Wake structure

Visualisations of the wake left behind by the falling Möbius bands were obtained using fluorescent dye (fluorescein), which was painted on the body prior to its release in the water tank. An example is shown in Fig. 7 for the small ring. The dye washes off the ring, still visible at the bottom of Fig. 7(a), as it falls, thus revealing qualitatively the vortical structures in the wake. The vertical distance travelled by the ring during one oscillation cycle is shown by a white bar in these figures. In Fig. 7(a), one can identify the large-scale arc of the helical trajectory [see Fig. 4(a) for comparison], as well as a fair number of smaller structures. At later times, these appear to evolve into larger ones which resemble vortex rings. Such rings have already been observed to be a central feature of the wake of other rising or falling bodies, such as spheres, undergoing vortex-induced oscillations (Horowitz and Williamson, 2008). Despite the complexity of the dye pattern, a vertical spacing of the wake structures approximately equal to the wavelength associated with the ring oscillations can be seen, which further illustrates the interaction between these oscillations and the vortices in the wake of the Möbius strip.

These visualisations show that already at fairly low Reynolds numbers (Re = 130 for the small band in Fig. 7), the flow generated by a freely falling Möbius strip is extremely complicated, even if the resulting body motion can be

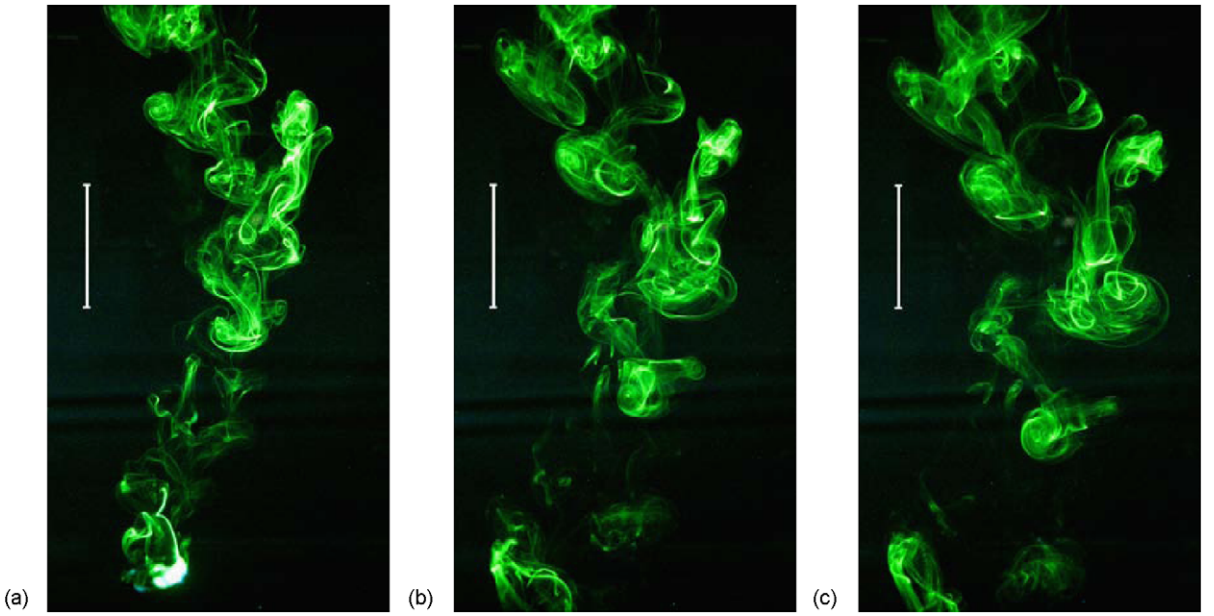

Fig. 7. Dye visualisations showing the development of the wake left behind by the small Möbius band (Re = 130). Images were taken at intervals of 5 s = 44 $d/U = 9.7\ D/U$. The white bars correspond to the distance U/f_v.

decomposed into two relatively simple ingredients. This would probably represent a considerable challenge for numerical simulations, in addition to the technical problems related to the meshing of such a topologically non-trivial object.

4. Conclusion

In this paper, we present a set of first results on the problem of a freely falling Möbius band, obtained from experiments in water at low Reynolds numbers. The two plastic bands used in this study have an intermediate perimeter-to-width ratio of 14, they differ in their mass coefficients and Reynolds numbers during the fall.

Both Möbius bands exhibit a similar behaviour in free fall. After their release they rapidly align in a direction at about 30° to the vertical, with their blunt edge facing down. Their motion can be decomposed into two relatively simple elements: (1) a large-scale helical trajectory, accompanied by a simultaneous rotation around the vertical, whose handedness and direction of rotation depend on the positive or negative twist of the band; and (2) a tilting or pitching oscillation, with lateral displacements of several body widths, induced by the vortical structures shed from the bluff leading ring element. Qualitative and quantitative measurements illustrating this behaviour were obtained from visualisations of the ring motion and wake flow.

An extension of this initial study would include a more systematic variation of the different parameters (aspect ratio, Reynolds number, mass coefficient), in order to identify their precise influence on the observed phenomena. Results concerning the wake of a fixed Möbius ring could also be useful in this respect.

Acknowledgement

The support of an Australian Research Council International Linkage Grant (LX0668992) is gratefully acknowledged.

References

Andersen, A., Pesavento, U., Wang, Z.J., 2005. Unsteady aerodynamics of fluttering and tumbling plates. Journal of Fluid Mechanics 541, 65–90.

Augspurger, C.K., 1986. Morphology and dispersal potential of wind-dispersed diaspores of neotropical trees. American Journal of Botany 73, 353–363.

Belmonte, A., Eisenberg, H., Moses, E., 1998. From flutter to tumble: inertial drag and Froude similarity in falling paper. Physical Review Letters 81, 345–348.

Dupleich, P., 1941. Rotation in free fall of rectangular wings of elongated shape. NACA Technical Memorandum 1201.

Fernandes, P.C., Ern, P., Risso, F., Magnaudet, J., 2005. On the zigzag dynamics of freely moving axisymmetric bodies. Physics of Fluids 17, 098107.

Field, S., Klaus, M., Moore, M.G., Nori, F., 1997. Chaotic dynamics in falling disks. Nature 388, 252–254.

Horowitz, M., Williamson, C.H.K., 2006. Dynamics of a rising and falling cylinder. Journal of Fluids and Structures 22, 837–843.

Horowitz, M., Williamson, C.H.K., 2008. Critical mass and a new periodic four-ring vortex wake mode for freely rising and falling spheres. Physics of Fluids 20, 101701.

Jenny, M., Dušek, J., Bouchet, G., 2004. Instabilities and transition of a sphere falling or ascending freely in a Newtonian fluid. Journal of Fluid Mechanics 508, 201–239.

Listing, J.B., 1861. Der Census räumlicher Complexe oder Verallgemeinerungen des Euler'schen Satzes von den Polyëdern. Abhandlungen der Königlichen Gesellschaft der Wissenschaften zu Göttingen, Mathematische Klasse 10, 97–182.

Lugt, H.J., 1983. Autorotation. Annual Review of Fluid Mechanics 15, 123–147.

Magnaudet, J., Eames, I., 2000. The motion of high-Reynolds-number bubbles in inhomogeneous flows. Annual Review of Fluid Mechanics 32, 659–708.

Mahadevan, L., Keller, J.B., 1993. The shape of a Moebius band. Proceedings of the Royal Society London A 440, 149–162.

Mahadevan, L., Ryu, W.S., Samuel, A.D.T., 1999. Tumbling cards. Physics of Fluids 11, 1–3.

Maxwell, J.C., 1990. In: Harman, P.M. (Ed.), The Scientific Letters and Papers of James Clerk Maxwell, vol. 1. Cambridge University Press, Cambridge, UK pp. 1846–1862.

Möbius, A.F., 1865. Über die Bestimmung des Inhaltes eines Polyeders. Berichte über die Verhandlungen der Königlichen Sächsischen Gesellschaft der Wissenschaften, Mathematisch-Naturwissenschaftliche Klasse 17, 31–68.

McCutchen, C.W., 1977. The spinning rotation of ash and tulip tree samaras. Science 197, 691–692.

Pesavento, U., Wang, Z.J., 2006. Falling paper: Navier–Stokes solutions, model of fluid forces, and center of mass elevation. Physical Review Letters 93, 144501.

Schwarz, G.E., 1990. The dark side of the Moebius strip. American Mathematical Monthly 97, 890–897.

Smith, E.H., 1971. Autorotating wings: an experimental investigation. Journal of Fluid Mechanics 50, 513–534.

Starostin, E.L., Van der Heijden, G.H.M., 2007. The shape of a Möbius strip. Nature Materials 6, 563–567.

Wang, Z.J., 2005. Dissecting insect flight. Annual Review of Fluid Mechanics 37, 183–210.

Willmarth, W.W., Hawk, N.E., Harvey, R.L., 1964. Steady and unsteady motions and wakes of freely falling disks. Physics of Fluids 7, 197–208.